

Effect of symmetry on electronic DOS, peierls transition and elastic modulus of carbon nanowires

C.H.Wong¹, J. Y. Dai², E. A. Buntov¹, V. N. Rychkov¹, M. B. Guseva³, A. F. Zatsepin^{1*}

¹*Institute of Physics and Technology, Ural Federal University, Ekaterinburg, 620002, Russia*

²*Department of Applied Physics, The Hong Kong Polytechnic University, Hong Kong, China*

³*Faculty of Physics, Moscow State University, Moscow, 119991 Russia*

* Corresponding author: Tel: (+73) 433754692; E-mail: a.f.zatsepin@urfu.ru

Received: 29 December 2016, Revised: 12 January 2017 and Accepted: 09 April 2017

DOI: 10.5185/amlett.2017.1578

www.vbripress.com/aml

Abstract

A Monte Carlo arithmetic method is utilized to investigate the Peierls transition in the linear and circular carbon nanowire respectively. The carbon nanowires interacting with the 6 nearest neighbors in hexagonal structure are spaced by 0.3 nm. Despite the Peierls transition of the linear carbon nanowires is unaffected by the Van der Waal's force, we discovered that the Peierls transition temperature of the isolated curved nanowire is raised to 910K under curvature. Based on the simulation results, the fluctuation of the atomic position of the atoms are stronger near to the free end boundary condition. Applying stress on the interstitial doped carbon nanowire array examines the elastic modulus which shows above 6TPa. The geometrical effect on the electronic density of states of the kink structural carbon chain is simulated by Harris functional in combination with Local Density Approximation. Two different lengths of branches A and B , are occupied alternatively to generate the asymmetric carbon chain. The ratio of the asymmetric branch length, $R_{AB} = A / B$, plays an important role in the electronic density of states DOS around Fermi level E_F . The highest DOS(E_F) occurs if the R_{AB} equals to 2 and while the Fermi level coincides with the Von-Hove singularity at $R_{AB} = 3$. Copyright © 2017 VBRI Press.

Keywords: Carbyne, symmetry, monte carlo, elastic moduli, Peierls transition.

Introduction

The great versatility and wide application of carbon materials arises from the strong dependence of their physical properties on the ratio of sp^1 (carbyne-like), sp^2 (graphite-like) to sp^3 (diamond-like) bonds. One dimensional sp^1 structures are being studied both experimentally and numerically, as their physical and chemical properties have prospective application in nanoelectronics, protective coatings, etc. One of the important developments in the field is the ion-assisted condensation of carbyne-like sp^1 chains, in-plane ordered in a hexagonal structure with nearly 5 angstroms interchain distance and held by Van-der-Waals forces [1]. This material can be produced in macroscopic volume and potentially finds a wide range of applications from microelectronics to medical implants [2-4]. Metal and semiconductor are indispensable ingredients from computer technology's point of view. The former such as Palladium serves as hard drives and circuit board components while the latter can be used as junction transistors. The fabulous electronic application is affirmed in the single walled carbon nanotube because it behaves

as either metal or semiconductor [5]. Similarly, the metal-semiconductor transformation is also possible theoretically in the carbon nanowire. The isolated carbon chain remains in metallic state below 500K but it becomes a semiconductor above 500K theoretically [6]. Carbon nanowire may become an emerging electronic device as the metal-semiconductor transition upon heating [6]. This interesting behavior triggers us to tune the Peierls transition temperature of the carbon nanowire. The new carbon structure in form of nanowire may hold a large elastic modulus as well [7, 8] and therefore it is a valuable to predict how large the elastic modulus of the carbon nanowire can be pushed upward under interstitial doping.

Finding a superconducting material in which the Fermi level is coincided to the Von Hove singularity point in electronic density of states is very rare. According to BCS theory, the superconducting transition temperature is proportional to the electronic density of states at Fermi level. Therefore, closing the gap between the Fermi-level and Von Hove singularity point is very important for high temperature superconductors [9, 10]. The tunable superconductivity is recently verified experimentally in

carbon nanotube [9]. However, the Fermi level and the singularity point may be widely separated in some superconductors. It is challenging to apply sufficient gate voltage or pressure to shift the Fermi level to the singularity point in nanomaterials [9]. As a result, we aim at discovering new materials in which the Fermi level is coincided with the singularity point and hopefully strengthens the electron phonon interaction of the carbon nanowire to create a new member of superconductors.

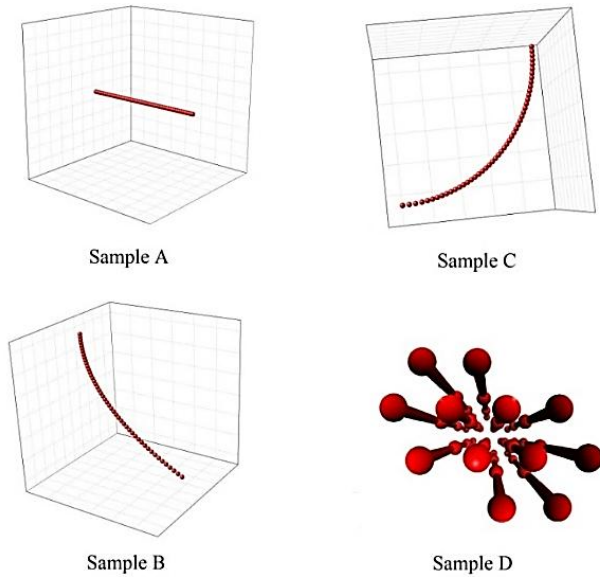


Fig. 1. The configurations of carbon nanowire at initial condition of the Monte Carlo simulation. Sample A is the isolated linear carbon chain. The curvature of sample B is weaker than sample C. Sample D is the coupled linear carbon chains. The lateral interaction between the nanowires in the sample D is the Van der Waal's force. Each nanowire carries 50 atoms.

Simulation method

The Hamiltonian of the linear carbon nanowire array is listed below [11].

$$H = e^{-T/T_{bj}} \sum_{m=1}^M \sum_{n=1}^{N-1} \left| E_{m,n,j} e^{-\frac{(r_{m,n}^{eq} - l_{m,n,j}^{eq})}{0.5 r_{m,n,j}^{eq}}} - E_2 \right| + e^{-T/T_{bj}} \sum_{m=1}^M \sum_{n=1}^{N-1} J_A (\cos \theta + 1)^2 - 4\varphi \left[\sum_{n,m} \left(\frac{\sigma}{r} \right)^6 - \left(\frac{\sigma}{r} \right)^{12} \right]$$

where T , E_2 , M , N are temperature, double bond energy, total number of chains, the total number of carbon in each chain, respectively. No metropolis iteration is operated at the first atom. The single, double and triple bond are named as $j = 1, 2$ and 3 respectively and the j is a stochastic variable. The r is spatial coordinate and $r_{m,n,j}^{eq}$ is equilibrium position. For instance, $r_{3,15,2}^{eq}$ refers to the

equilibrium location of 15th atom along 3th chain with double bond connection. For linear carbon chain the $(\cos \theta + 1)^2$ is zero. The angular energy J_A is 600 kJ/mol but the true angular energy in various θ will be weakened by $(\cos \theta + 1)^2$ [11]. The bond softening temperature of the covalent bond T_{bj} [11] is calculated by $E_j = k_B T_{bj}$ where Boltzmann constant $k_B = 1.38 \times 10^{-23} JK^{-1}$. The Van der Waal's force is the only interaction between the adjacent nanowires and the φ and σ are $8.1 \times 10^{-23} J$ and $1.23 \times 10^{-10} m$ respectively [11]. The single bond, double bond and triple bond energy are 348 kJ/mol, 614 kJ/mol and 839 kJ/mol at room temperature respectively [12]. The $C-C$, $C=C$ and $C \equiv C$ bond distance are $r_{m,n,1}^{eq} = 154$ pm, $r_{m,n,2}^{eq} = 134$ pm and $r_{m,n,3}^{eq} = 120$ pm [12]. Periodic boundary condition is applied along the lateral plane to grantee each nanowire in the sample D has 6 nearest neighbors.

The orthogonal vibration of the atoms in the linear nanowire is relative to the pivot angle of 180 degree. However, the transverse vibration of the atoms is relative to $180 - \varphi$ degree in the case of curved chain. In other word, the angular energy of the circular nanowire will be strengthened depending on how strong the curvature is. We follow the same algorithm [11] to investigate the isolated circular carbon nanowires with the same number of atoms. The complexity is reduced because the Van Der Waal's force is disappeared in the isolated nanowire. The atomic vibrations of the curved nanowire are resolved into three components in cylindrical coordinate (ρ, φ, z) similarly, one longitudinal $(\rho d\varphi = dl)$ and two transverse directions $(d\rho \& dz)$. Due to the strong covalent bond, the movement of the atoms along the transverse direction is much weaker than the longitudinal vibrations and hence [11]

$$dz = d\rho = \frac{k_B T}{(E_{m,n,1} + E_{m,n,2} + E_{m,n,3})/3} dl$$

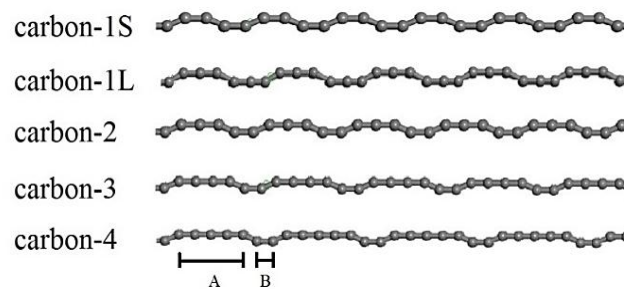


Fig. 2. All carbon are connected by double bond length of 134pm and the kink angle is 30 degree (unless otherwise specified). For clarity reason, only 8 basis are shown here. The symmetric branch length of 134pm and 268pm are named as carbon-1S and carbon-1L respectively with $R_{AB} = 1$. The asymmetric branch ratio, R_{AB} of 2, 3 and 4, refers to carbon-2, carbon-3 and carbon-4 respectively.

The additional work done due to mechanical force is needed added into the Hamiltonian in order to compute in the elastic modulus along the chain axis [11]. Interstitial dopants will decrease the atomic mean free path of carbon based on the particle concentration. Assume the dopants are chemically unreactive and distributed randomly beside the nanowires. The atomic mean free path is inversely proportional to the cube root of particle concentration. The density of state of electron of the infinite long carbon chain are determined by the Dmol³ package in Material-Studio 7 in which the Harris functional and Local Density Approximation (LDA) are taken into account [13-16] in order to reduce computational cost.

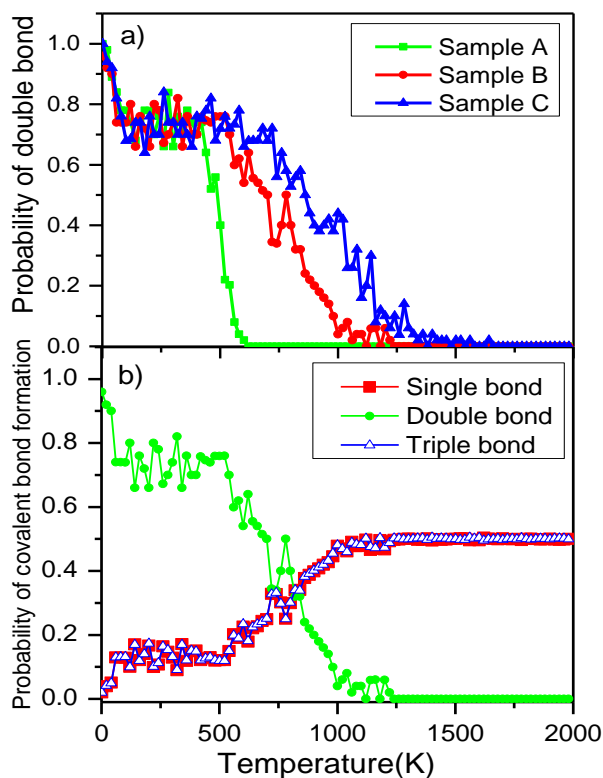


Fig. 3. (a) The curvature-assisted Peierls transition temperature is observed. The phase transition is broader under curvature. The Peierls transition temperature (the mid-point in the transient region) of the sample A, B and C are 500, 742 and 910K respectively. (b) The distribution of different types of covalent bonds as a function of temperatures. At 0K, all carbon atoms in the sample D are connected by double bond. Thermal effect triggers more single and triple bond to exist in equally weighted. The Peierls transition occurs at 500K.

Results and discussion

Fig. 3a demonstrates that the Peierls transition temperature is increased with curvature. The polyvne phase in the sample B and C is formed completely if the temperature rises to 1250K and 1500K respectively. This phenomenon can be explained by the recent study of the carbon nanowire which shows that the Peierls transition temperature is enhanced by the shortening of the atomic mean free path [11]. The circular geometries of the sample B and C are likely induced the radial and tangential component of the atomic vibrations and

therefore the scattering surface of the atom is larger to cause the atomic motion more difficulty. Moreover, the curvature serves as a geometrical constraint which perturbs the atomic movement due to the angular energy term. The sample A shows the sharpest transition because all atoms allow rearranging the new coordinates consistently in the absence of the perturbation from the angular energy.

Fig. 4 displays the simulation results of the sample C at room temperature. The transverse vibration is rare at the 1st atom. However, if the atoms locate further away from the bottom, the transverse fluctuations turn into more vigorously. It is owing to the one end fixed boundary condition at the 1st atom. In the extreme case, the 50th atom is hold by one side of spring constant only and it is relatively free in term of motion [17]. In contrast, the 2nd atom cannot push the 1st atom due to the fixed boundary condition. Worse still, the 2nd atom is holding back by the other 48 atoms in a row that make the atomic dynamics almost impossible [17]. If the longitudinal interaction is weaker at the free end, the noise arising from the transverse interaction is easier to emerge to spread the atoms [17]. The argument is also applicable to the sample B. The Peierls transition of the sample D takes place at 500K which is located at the middle of the transient zone as illustrated in Figure 3b. The ratio of the single to triple bond is almost identical at any temperature.

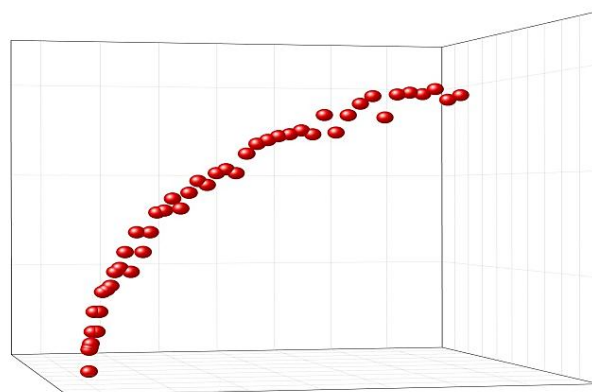


Fig. 4. The example of simulation results of the sample C (RHS) at 300K. The red balls represent atomic coordinate of the carbon atoms. After geometrical translation of the first atom for better readability, the first atom is located at the bottom. The same translation vector applies to shift the other atoms correspondingly. The average bond distance of the sample B and C is 134.8pm and 136.4pm respectively. The simulation results of sample A can be found in C.H. Wong *et al.* [11].

The phase transition from the cumulene to polyvne is completed at 600K by the disappearance of the double bond. In comparison to the reduction of the double bond in Figure 3a, the Van Der Waal's force does not affect the Peierls transition temperature based on the devastation of the double bond as a function of temperatures in sample A and D [11]. We confirm that the Van der Waal's force is not strong enough to alternate the Peierls transition temperature in our provided sample. The elastic modulus of the coupled carbon array is reinforced by interstitial

dopants as shown in **Fig. 5**. The elastic modulus is increased from 5.1 to 6.3 TPa linearly if the doping level is up to 20% because the dopants restrict the atomic motion [17].

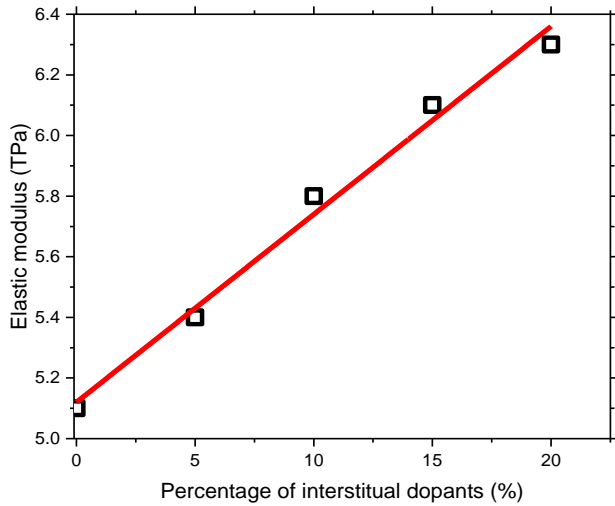


Fig. 5. The elastic modulus is increased by 24% in the present of interstitial dopants.

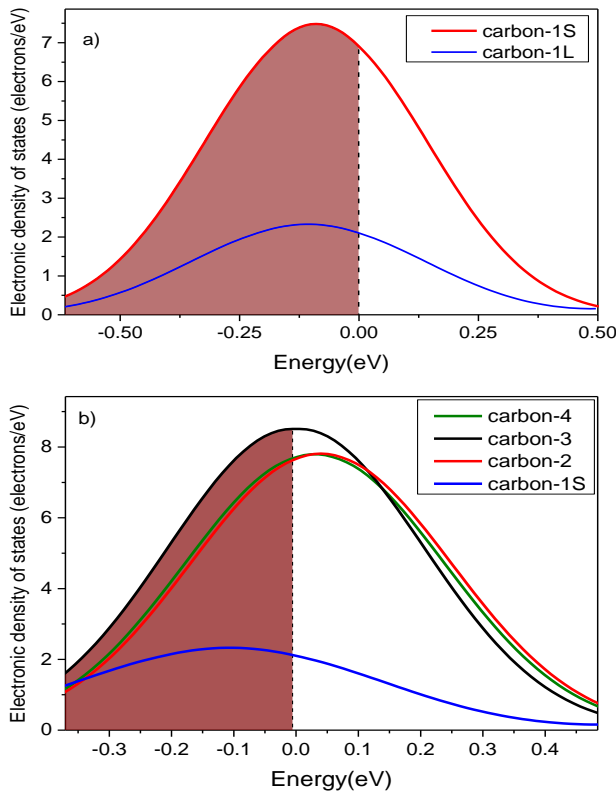


Fig. 6. (a) The electronic density of states DOS in the symmetric carbon chains. The Fermi-level is shifted to 0 eV for convenience. The shaded region refers to the filled states. (b) The electronic density of state of the carbon chains in various R_{AB} . The Fermi-level is adjusted to 0 eV for better readability.

The DOS of the symmetric carbon chains as a function of electron energies under $R_{AB} = 1$ is compared in **Fig. 6a**. Increasing the branch length symmetrically from

134pm to 268pm pushes the $DOS(E_F)$ about 2.3 times higher. Their Von-Hove singularity points [18, 9] in the DOS almost align at the same electron energy and therefore it is ineffective to move the Fermi-level to the singularity point by tuning the branch length symmetrically. Figure 8 provides a predominant method to close the gap between the Fermi-level and singularity point by adjusting the branch length asymmetrically. In case of $R_{AB} \neq 1$, the E_F of the carbon chains are much closer to the Von Hove singularity points when compared to the symmetric case. The $DOS(E_F)$ of $R_{AB} = 3$ coincides with the singularity point which is an appreciative phenomenon to enhance the electron phonon coupling. The $DOS(\text{peak})$ also move in a similar manner based on the GGA functional of the CASTEP. However, the most effective way to strengthen the electron phonon coupling is likely to push the Fermi level by 0.06eV in the carbon-2. In general, the $DOS(E_F)$ of the symmetric carbon chain is the lower than the asymmetric nanowire as shown in **Fig. 6** and **Table 1**.

Table 1. Compare the ratio of the DOS at Fermi level relative to the linear carbon chain.

	R_{AB} (relative to 134pm)	$DOS(E_F)$
carbon-1S	1	0.52
carbon-2	2	1.53
carbon-3	3	1.42
carbon-4	4	1.09

Conclusion

Despite the Van Der Waal’s force shows no influence on the Peierls transition temperature of the carbon nanowire, the increase of the Peierls transition temperature from 500 K to 910 K is observed under curvature. A weak reinforcement in the elastic modulus of the carbon chain is confirmed by the Monte Carlo method at various levels of interstitial doping. The atomic coordinate of the carbon atoms at equilibrium along the short nanowire is disturbed by the boundary condition. The carbon atoms occupied denser at the fixed boundary case. On the other hand, we have investigated the electronic density of states of the carbon chain under symmetric and asymmetric branch. Instead of compressing the sample or injecting gate voltage, a guideline of tuning the Fermi level to the Von-Hove singularity in the electronic density of state is provided by kink structure. According to our simulation, closing the gap between the Fermi-level and the Von-Hove singularity by the generation of asymmetric kink structure is more wisely than the design of symmetric carbon chain. Interestingly the Fermi-level of the carbon chain is intrinsically aligned at the Von-Hove singularity if the ratio of the asymmetric branch length is 3 (relative to 134pm).

Acknowledgements

The research was supported by Act 211 of the Government of the Russian Federation, contract no. 02. A03.21.0006.

References

1. Babaev, V.; Guseva, M.; Khvostov, V. et al. Carbon Material with Highly Ordered Linear-Chain Structure, in "POLYYNES - Synthesis, Properties, Applications"; edr. Fr.Cataldo, CRC press - USA, **2005**, pp. 219-252.
DOI: [10.1201/9781420027587.ch11](https://doi.org/10.1201/9781420027587.ch11)
2. Guseva, M.; Babaev, V.; Novikov, N.; US Patent 6355350 B1, **2002**.
3. Guseva, M.; Babaev, V.; Novikov, N.; US Patent 6454797 B2, **2002**.
4. Guseva, M.; Babaev, V.; Novikov, N.; US Patent 6555224 B2, **2003**.
5. Rossouw, D.; Botton, G.; Najafi, E.; Lee, V. and Hitchcock, A.; ACS Nano, **2012**, *6*, 10965.
DOI: [10.1021/nn3045227](https://doi.org/10.1021/nn3045227)
6. Liu, X.; Zhang, G.; Zhang, Y.-W.; J. Phys. Chem. C, **2015**, *119*, 24156.
DOI: [10.1021/acs.jpcc.5b08026](https://doi.org/10.1021/acs.jpcc.5b08026)
7. Kotrechko, S.; Mikhailovskij, I.; Mazilova, T.; Sadanov, E.; Timoshevskii, A.; Stetsenko, N.; Matviychuk, Yu.; Nanoscale Res. Lett., **2015**, *10*, 24.
DOI: [10.1186/s11671-015-0761-2](https://doi.org/10.1186/s11671-015-0761-2)
8. Liu, M., Artyukhov, V.; Lee, H.; Xu, F.; Yakobson, B.; ACS Nano, **2013**, *7*, 10075.
DOI: [10.1021/nn404177r](https://doi.org/10.1021/nn404177r)
9. Yang, Y.; Fedorov, G.; Shafranjuk, S.; Klapwijk, T.; Cooper, B.; Lewis, R.; Lobb, C.; Barbara, P.; Nano Lett., **2015**, *15*, 7859.
DOI: [10.1021/acs.nanolett.5b02564](https://doi.org/10.1021/acs.nanolett.5b02564)
10. Altomare, F.; Chang, A.; One-Dimensional Superconductivity in Nanowires, Wiley:USA, **2013**.
DOI: [10.1002/9783527649044](https://doi.org/10.1002/9783527649044)
11. Wong, C.; Buntov, E.; Rychkov, V.; Guseva, M.; Zatsepin, A.; Carbon, **2017**, *114*, 106.
DOI: [10.1016/j.carbon.2016.12.009](https://doi.org/10.1016/j.carbon.2016.12.009)
12. Laird, B.; University Chemistry, McGraw-Hill Science, ISBN-13: 978-0077221331, **2008**.
13. Cortez-Valadeza, M.; Fierrob, C.; Farias-Mancillab, J.; Vargas-Ortizc, A.; Flores-Acostaa, M.; Ramirez-Bone, R.; Enriquez-Carrejob, J.; Soubervielle-Montalvod, C.; Mani-Gonzalez, P.; Chemical Physics, **2016**, *472*, 81.
DOI: [10.1016/j.chemphys.2016.03.008](https://doi.org/10.1016/j.chemphys.2016.03.008)
14. Gritsenko, O.; Mentel, L.; Baerends, E.; J. Chem. Phys. **2016**, *144*, 204114. DOI: [10.1063/1.4950877](https://doi.org/10.1063/1.4950877)
15. Robertson, I.; Farid, B.; Phys. Rev. Lett., **1991**, *66*, 3265.
DOI: [10.1103/PhysRevLett.66.3265](https://doi.org/10.1103/PhysRevLett.66.3265)
16. Zaremba, E.; J. of Phys.: Condensed Matter, **1990**, *2*, 2479.
DOI: [10.1088/0953-8984/2/10/018](https://doi.org/10.1088/0953-8984/2/10/018)
17. Christman, J.; Fundamentals of solid state physics, Wiley: USA, **1988**.
18. Xu, S.; Liu, C.; Belopolski, I.; Kushwaha, S.; et al.; Phys. Rev. B, **2015**, *92*, 075115.
DOI: [10.1103/PhysRevB.92.075115](https://doi.org/10.1103/PhysRevB.92.075115)